

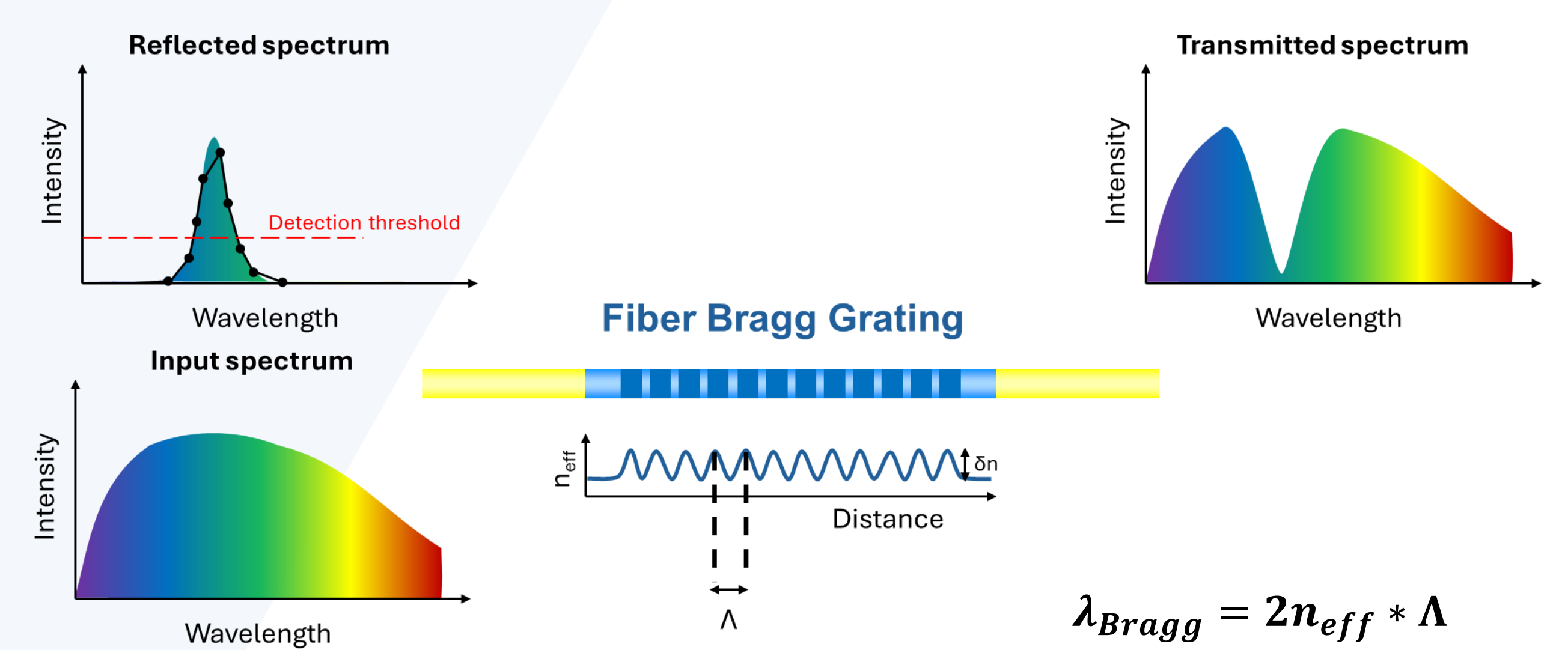
# Temperature and strain monitoring in Reykjanes geothermal field, Iceland, using quasi-distributed fiber-optic sensing

Julien Govoorts<sup>1,2,3</sup>, Corentin Caudron<sup>1,4</sup>, Jiaxuan Li<sup>5</sup>, Haiyang Liao<sup>5</sup>, Christophe Caucheteur<sup>2,4</sup>, Yesim Çubuk-Sabuncu<sup>6</sup>, Halldór Geirsson<sup>7</sup>, Vala Hjörleifsdóttir<sup>8</sup>, Kristín Jónsdóttir<sup>6</sup>, Loic Peiffer<sup>9</sup>

- 1. Département Géosciences, Environnement et Société, Laboratoire G-Time, Université libre de Bruxelles, Brussels, Belgium (julien.govoorts@ulb.be)
- 2. Department of Electromagnetism and Telecommunication, Advanced Photonic Sensors Unit, Université de Mons, Mons, Belgium
- 3. Seismology-Gravimetry, Royal observatory of Belgium, Uccle, Belgium
- 4. Wel-T Research Institute, Wavre, Belgium
- 5. Department of Earth and Atmospheric Sciences, University of Houston, Houston, United States
- 6. Icelandic Meteorological Office, Reykjavik, Iceland
- 7. Institute of Earth Sciences, University of Iceland, Reykjavik, Iceland
- 8. Reykjavik University, Reykjavik, Iceland
- 9. Departamento de Geología, Centro de Investigación Científica y de Educación Superior de Ensenada, Ensenada, Mexico



## • What's a Fiber Bragg Grating ?



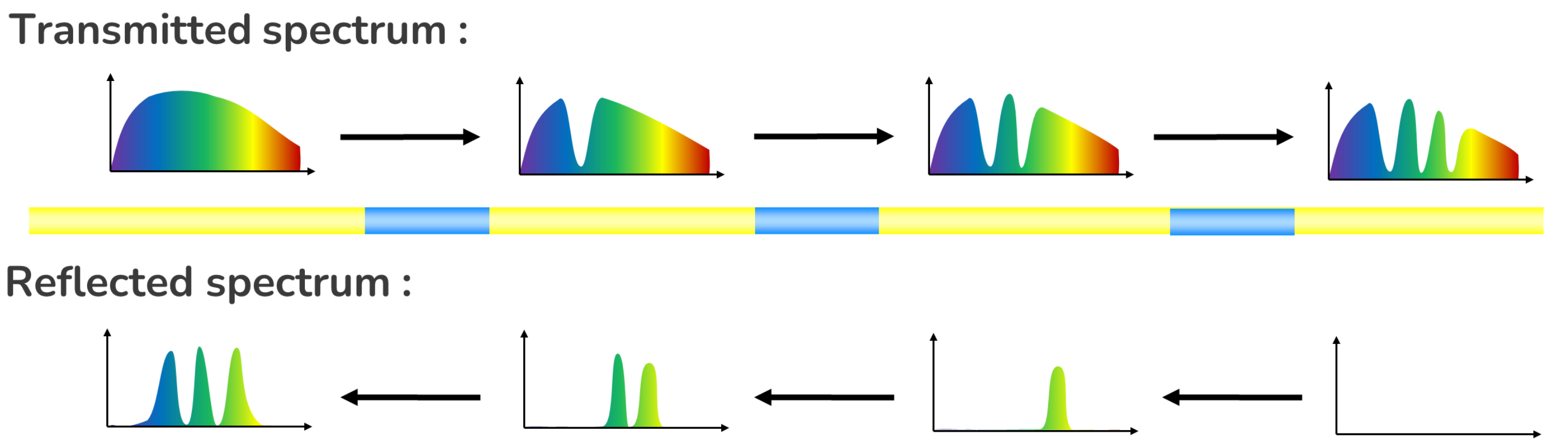
$$\lambda_{Bragg} = 2n_{eff} * \Lambda$$

A **Fiber Bragg Grating (FBG)** is a permanent and periodic ( $\Lambda$ ) change in the core refractive index ( $n_{eff}$ ) that leads to a **strong light reflection at a specific wavelength**.

Strain and temperature variations lead to changes in the refractive index and grating period ( $\Lambda$ ), causing a **wavelength shift** :

- 10 pm/°C
- 1.2 pm/ $\mu$ m

## • How to turn it into a quasi-distributed sensor ?



To turn the fiber-optic into a **quasi-distributed sensor**, Bragg reflectors are inscribed at **different wavelengths** and at **different locations**. Each FBG **reflects a portion of the spectrum** like a bandpass filter. Up to 20 FBGs can be connected on the same fiber!

The number of sensed fiber can be increased using an optical switch. Since each fiber is interrogated independently, **hundreds of FBGs can be sampled from the same interrogator!**

## • Comparison between Fiber Bragg Grating and the Distributed Acoustic Sensing

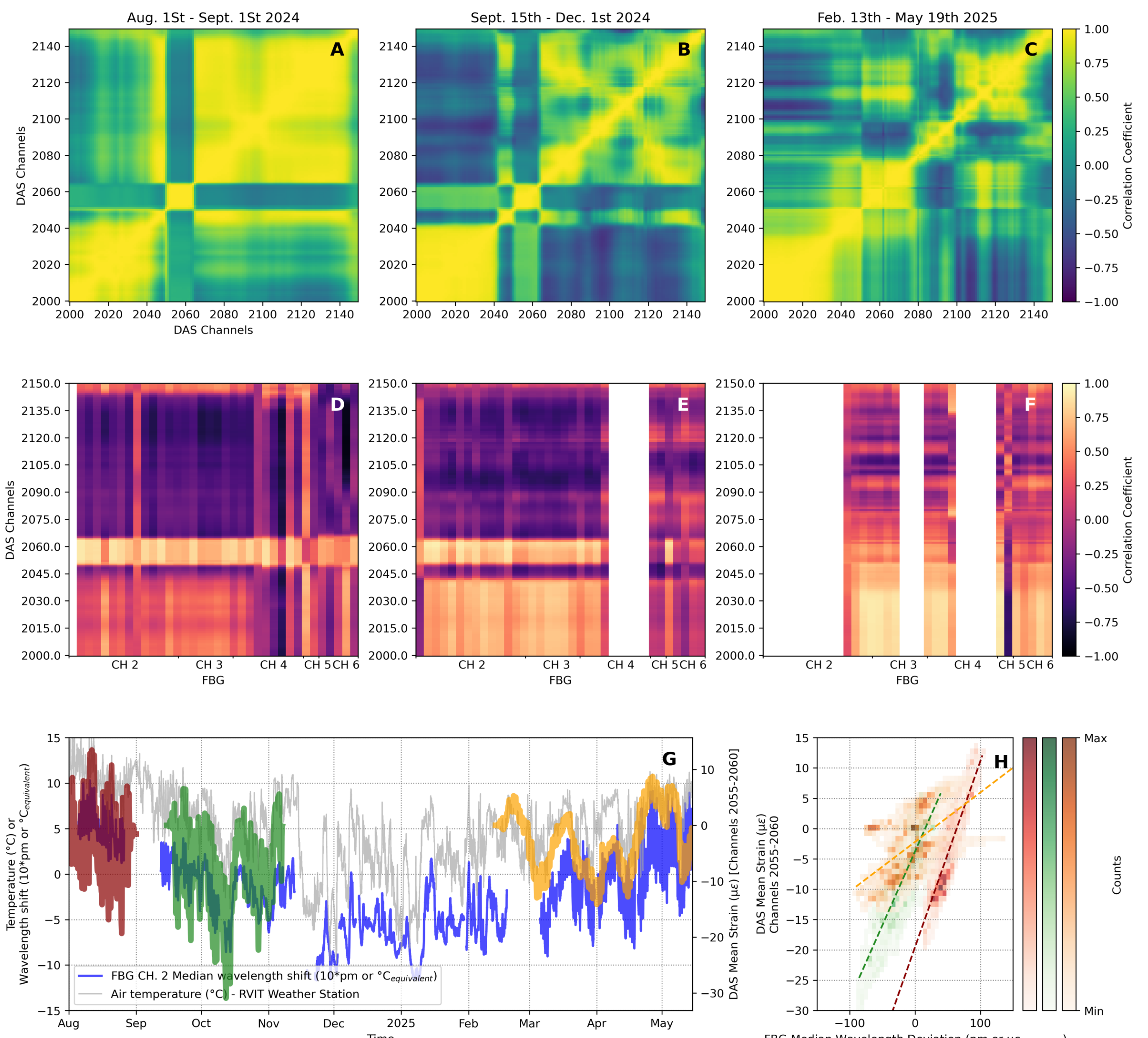


Fig. 1 : A, B and C : Correlation coefficient matrices of the DAS channels correlated with themselves for the different sensing periods. D, E, and F : Correlation coefficient between the DAS channels and the FBG sensors on the channels 2, 3, 4 and 6. G : Time series of the median wavelength shift over all the FBG temperature sensors on channel 2 (blue). Air temperature recorded at RVIT weather station located 1.5 km away from the deployment site (Grey). The red, green and yellow are corresponding to the strain obtained from the different DAS interrogation periods. H : Linear regressions between the median wavelength shift over all the FBG temperature sensors on channel 2 and the average strain over the DAS channels ranging from 2055 to 2060 for the 3 different sensing periods. The different colorscales correspond to the different sensing periods and match the line colors on the panel G.

The **FBG** and the section of a telecom fiber interrogated by a **Distributed Acoustic Sensing (DAS)** show **similarities** (Fig. 1). Some part of the **DAS data** are **well-correlated with FBG temperature sensors** which are air-temperature driven.

However, the correlation coefficients between the FBG and DAS, as well as within the DAS itself, are changing over time. **These changes occurred close to the 1<sup>st</sup> of April 2025 eruption!**

## • April 1st, 2025 Svartsengi Eruption

Observing the **ground deformation** using **FBG, DAS and GNSS** (Fig. 2) caused by a **volcanic eruption** !

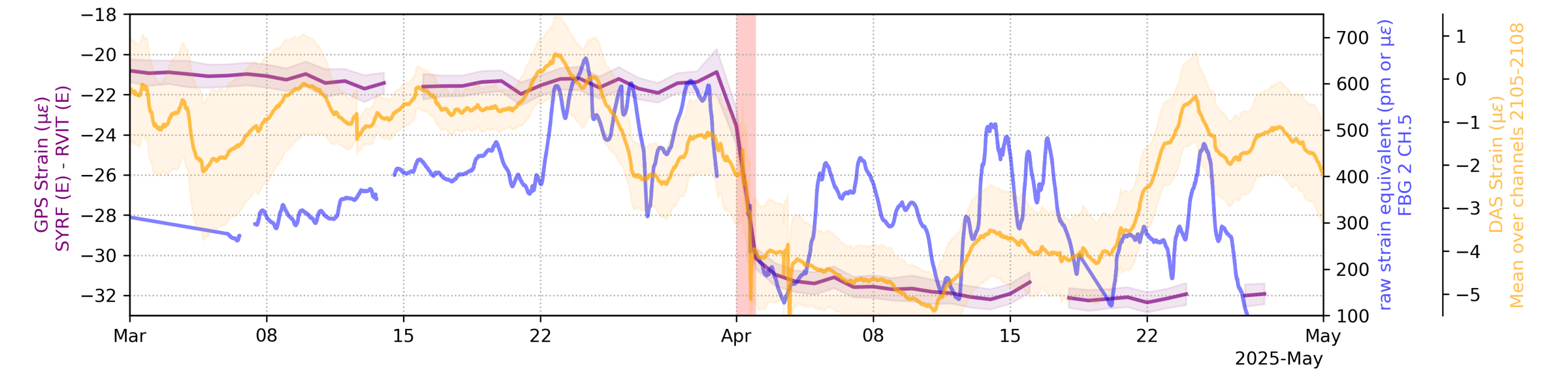


Fig. 2 : Strain recorded by the FBG strain-pad mounted diagonally on the channel 5 (blue) and the mean strain and its standard deviation gathered over the DAS channels 2105 - 2108 (orange). Computed strain from the GNSS stations for the east component and its error (purple). The red overlaid period corresponds to the eruption that occurred at Svartsengi on the 1<sup>st</sup> of April 2025. An abrupt change in strain is observed for the three different technologies deployed in the field.

## • Periodic signals :

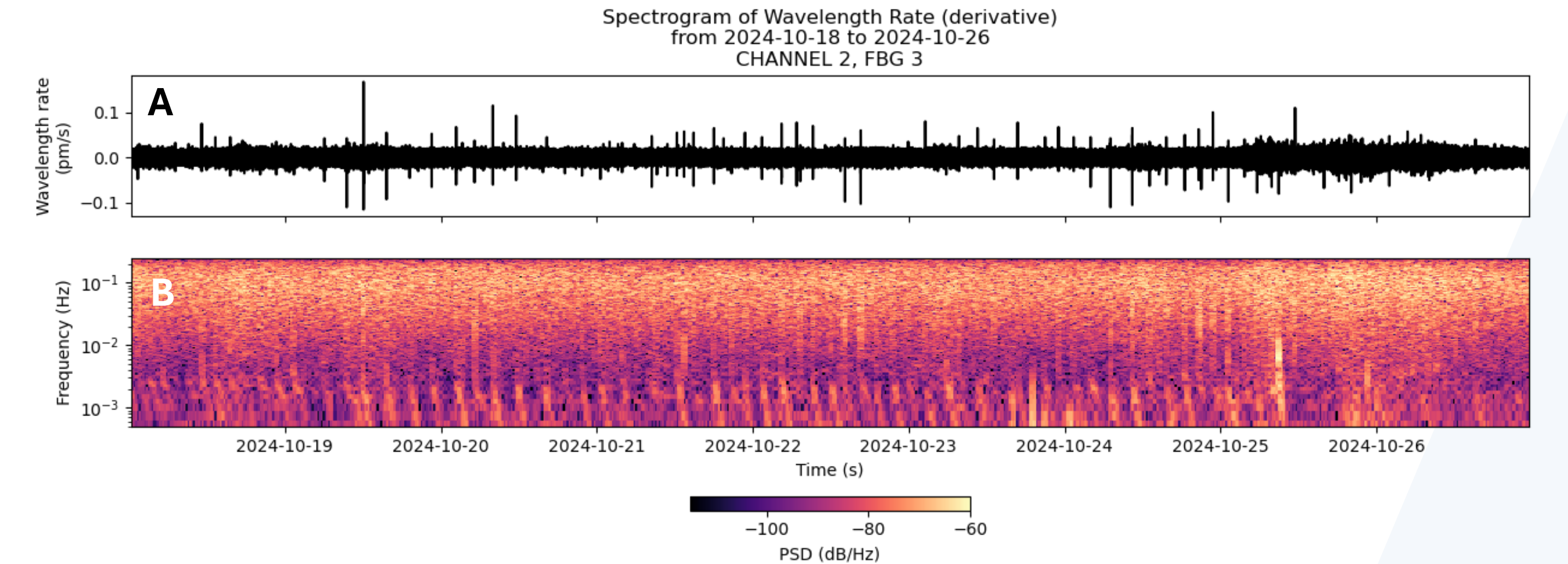


Fig. 3 : A : Time series in strain rate from the third FBG strain-pad located on channel 2 and installed horizontally in-ground between the October 18th, 2024, and October 26th, 2024. The signal shows periodic variation with a cycle length of 3 to 4 hours. B : Spectrogram of the above signal computed using 66-minute windows with 75% overlap.

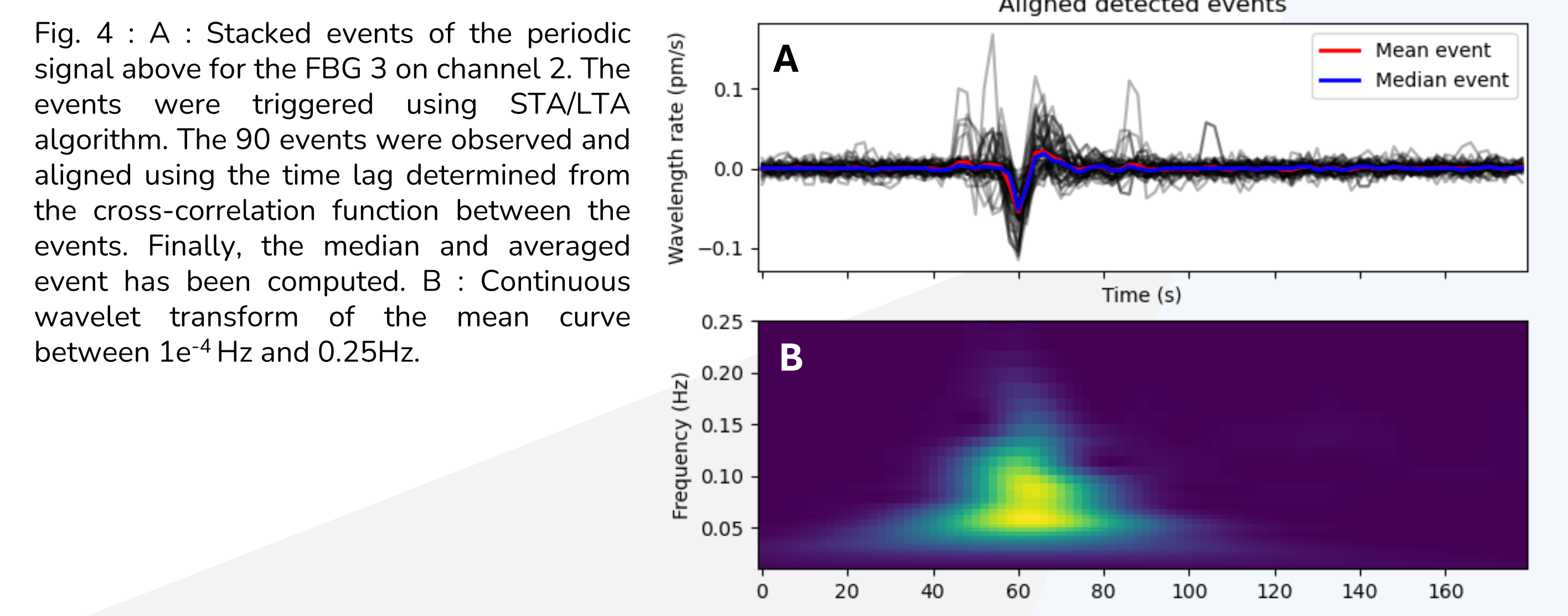


Fig. 4 : A : Stacked events of the periodic signal above for the FBG 3 on channel 2. The events were triggered using STA/LTA algorithm. The 90 events were observed and aligned using the time lag determined from the cross-correlation function between the events. Finally, the median and averaged event has been computed. B : Continuous wavelet transform of the mean curve between 1e<sup>-4</sup> Hz and 0.25Hz.

**Supplementary: Temperature and strain monitoring in Reykjanes geothermal field, Iceland, using quasi-distributed fiber-optic sensing**

Julien Govoorts, Corentin Caudron, Jiaxuan li, Haiyang Liao, Christophe Caucheteur, Yesim Çubuk-Sabuncu, Halldór Geirsson, Vata Hjörleifsdóttir, Kristín Jónsdóttir, Loic Peiffer

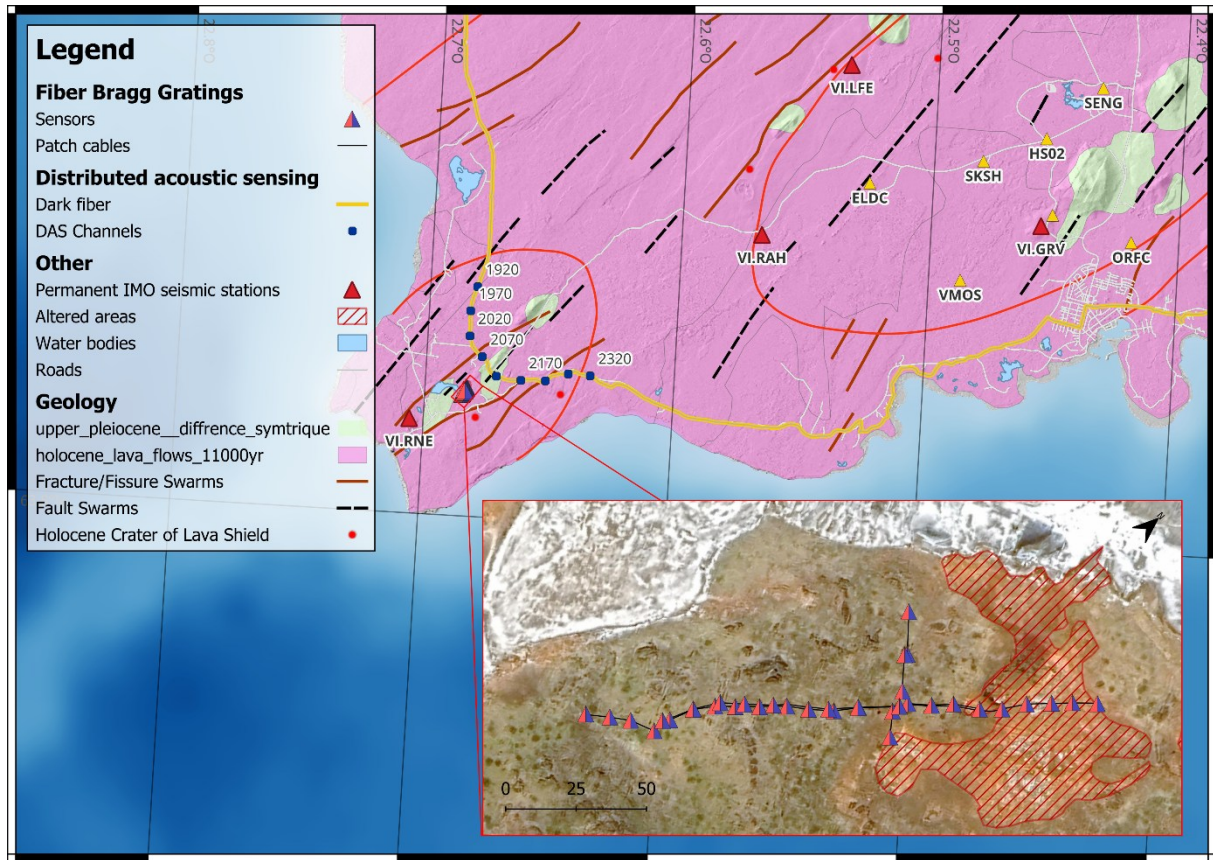


Figure 1 : Deployment map showing the locations of Fiber Bragg Grating sensors, dark telecom fiber (copyright: Li et al (2024) under Creative Commons Zero v1.0 Universal) sensed by a DAS and the GNSS permanent network. The deployment took place in the Reykjanes Peninsula in Iceland and more specifically at the Gunnhver geothermal area. Copyrights: Geological settings map : Náttúrufræðistofnun Íslands – Icelandic Institute of Natural History. Tekið saman af Hauki Jóhannessyni og Kristjáni Sæmundssyn retrieved on the April 30 2026 ; Location of the GNSS stations and seismic permanent network: Icelandic Meteorological Office - Veðurstofa Íslands under Attribution-ShareAlike 4.0 International (CC BY-SA 4.0) ; The satellite imagery : Google Inc, Google Satellite, retrieved on the April 30 2026.

**Supplementary: Temperature and strain monitoring in Reykjanes geothermal field, Iceland, using quasi-distributed fiber-optic sensing**

**Julien Govoorts**, Corentin Caudron, Jiaxuan li, Haiyang Liao, Christophe Caucheteur, Yesim Çubuk-Sabuncu, Halldór Geirsson, Vala Hjörleifsdóttir, Kristín Jónsdóttir, Loic Peiffer

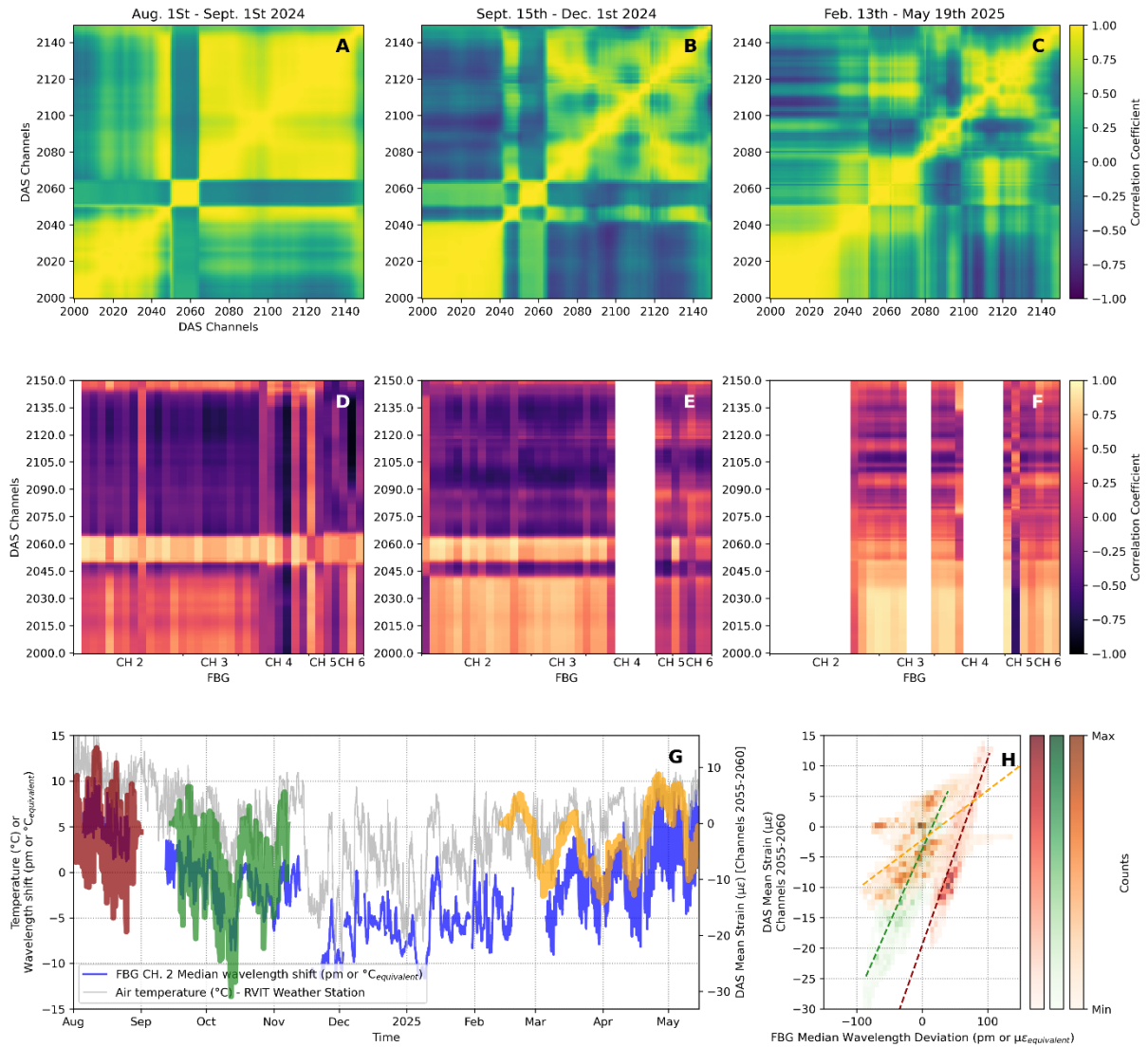


Figure 2: A, B and C : Correlation coefficient matrices of the DAS channels correlated with themselves for the different sensing periods. D, E, and F : Correlation coefficient between the DAS channels and the FBG sensors on the channels 2, 3, 4 and 6. G : Time series of the median wavelength shift over all the FBG temperature sensors on channel 2 (blue). Air temperature recorded at RVIT weather station (owned by Icelandic Road Administration) located 1.5 km away from the deployment site (Grey). The red, green and yellow are corresponding to the strain obtained from the different DAS interrogation periods. H : Linear regressions between the median wavelength shift over all the FBG temperature sensors on channel 2 and the average strain over the DAS channels ranging from 2055 to 2060 for the 3 different sensing periods. The different colorscales correspond to the different sensing periods and match the line colors on the panel G.

**Supplementary:** Temperature and strain monitoring in Reykjanes geothermal field, Iceland, using quasi-distributed fiber-optic sensing

**Julien Govoorts**, Corentin Caudron, Jiaxuan li, Haiyang Liao, Christophe Caucheteur, Yesim Çubuk-Sabuncu, Halldór Geirsson, Vala Hjörleifsdóttir, Kristín Jónsdóttir, Loic Peiffer

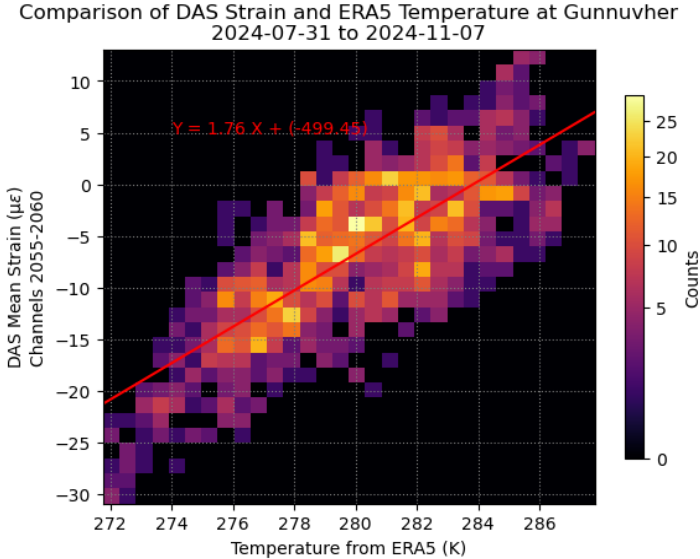


Figure 3 : Comparison between the averaged strain recorded on the channels 2055-2060 with the DAS and the ERA5 temperature reanalysis model (Copernicus Climate Change Service, 2023 ; Hersbach et al 2018).

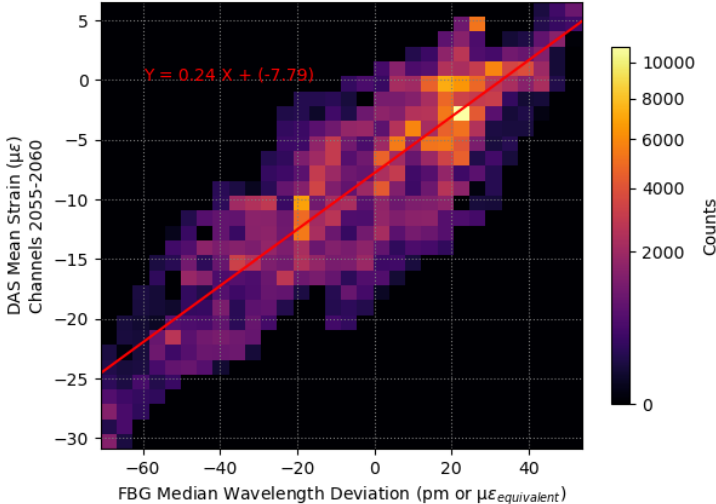


Figure 4 : Comparison between the averaged strain recorded on the channels 2055-2060 with the DAS and the wavelength shift gathered with the FBG on the channel 2.

**Supplementary:** Temperature and strain monitoring in Reykjanes geothermal field, Iceland, using quasi-distributed fiber-optic sensing

**Julien Govoorts**, Corentin Caudron, Jiaxuan li, Haiyang Liao, Christophe Caucheteur, Yesim Çubuk-Sabuncu, Halldór Geirsson, Vata Hjörleifsdóttir, Kristín Jónsdóttir, Loic Peiffer

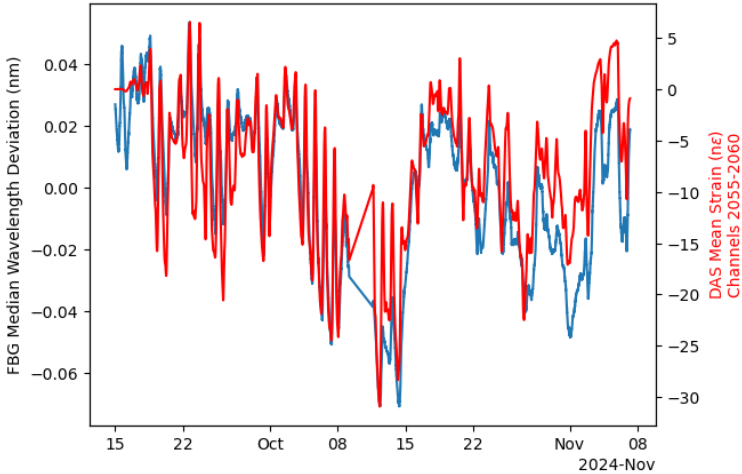


Figure 5 : Averaged strain time serie recorded on the channels 2055-2060 with the DAS and the wavelength shit time serie gathered with the FBG on the channel 2.

## Supplementary: Temperature and strain monitoring in Reykjanes geothermal field, Iceland, using quasi-distributed fiber-optic sensing

Julien Govoorts, Corentin Caudron, Jiaxuan li, Haiyang Liao, Christophe Caucheteur, Yesim Çubuk-Sabuncu, Halldór Geirsson, Vala Hjörleifsdóttir, Kristín Jónsdóttir, Loic Peiffer

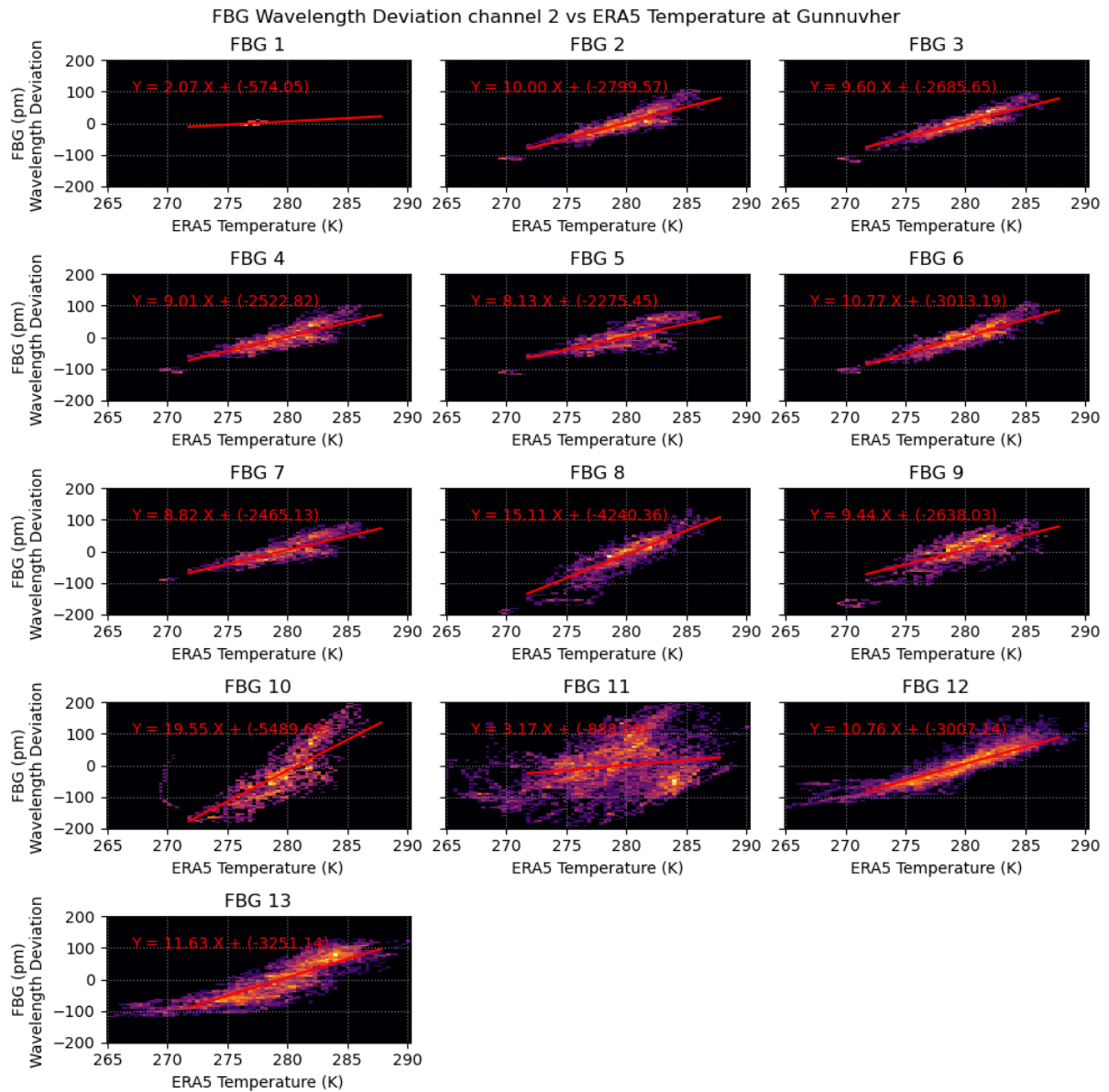


Figure 6 : Comparison between the wavelength shift from all the FBG located on channel 2 and the ERA5 temperature reanalysis model (Copernicus Climate Change Service, 2023 ; Hersbach et al 2018).

## Supplementary: Temperature and strain monitoring in Reykjanes geothermal field, Iceland, using quasi-distributed fiber-optic sensing

Julien Govoorts, Corentin Caudron, Jiaxuan li, Haiyang Liao, Christophe Caucheteur, Yesim Çubuk-Sabuncu, Halldór Geirsson, Vala Hjörleifsdóttir, Kristín Jónsdóttir, Loic Peiffer

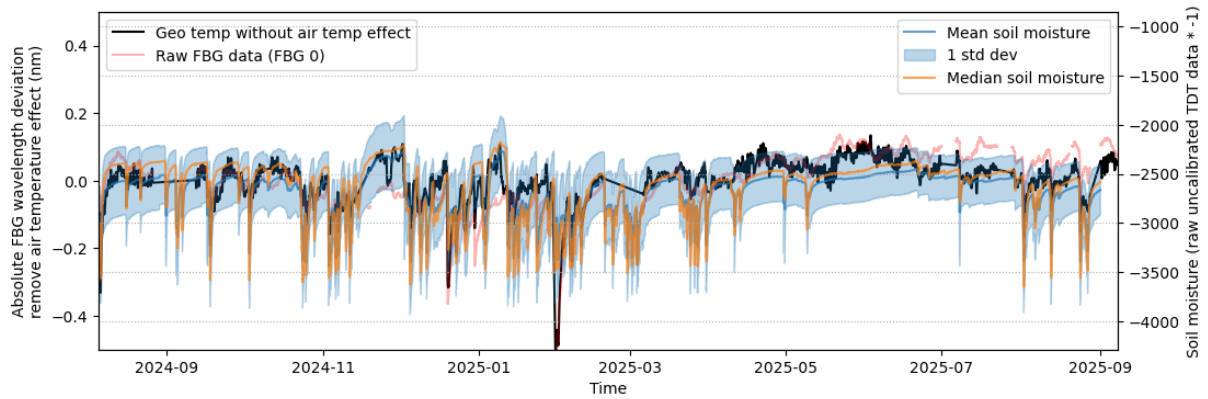


Figure 7 : Wavelength shift from the FBG 1 on channel 5 located near a steam vent (black and orange). The blue and orange curves are corresponding to the uncalibrated soil moisture retrieved from the TOMST sensors deployed on site.

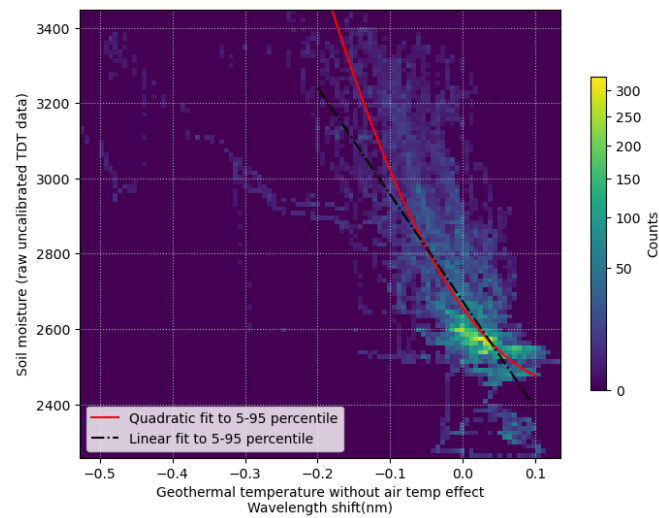


Figure 8 : Quadratic and linear regression between the temperature recorded from the FBG 1 on channel 5 after removing the air temperature effect and the soil moisture averaged over all the TOMST sensors deployed on site.

**Supplementary:** Temperature and strain monitoring in Reykjanes geothermal field, Iceland, using quasi-distributed fiber-optic sensing

**Julien Govoorts**, Corentin Caudron, Jiaxuan li, Haiyang Liao, Christophe Caucheteur, Yesim Çubuk-Sabuncu, Halldór Geirsson, Vala Hjörleifsdóttir, Kristín Jónsdóttir, Loic Peiffer

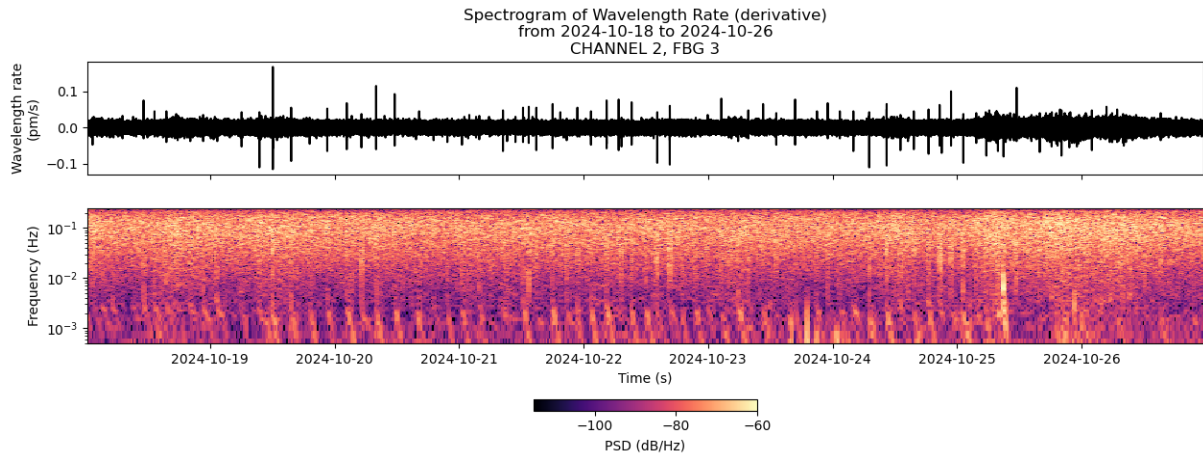


Figure 9 : Time series in strain rate from the third FBG strain-pad located on channel 2 and installed horizontally in-ground between the October 18th, 2024, and October 26th, 2024. The signal shows periodic variation with a cycle length of 3 to 4

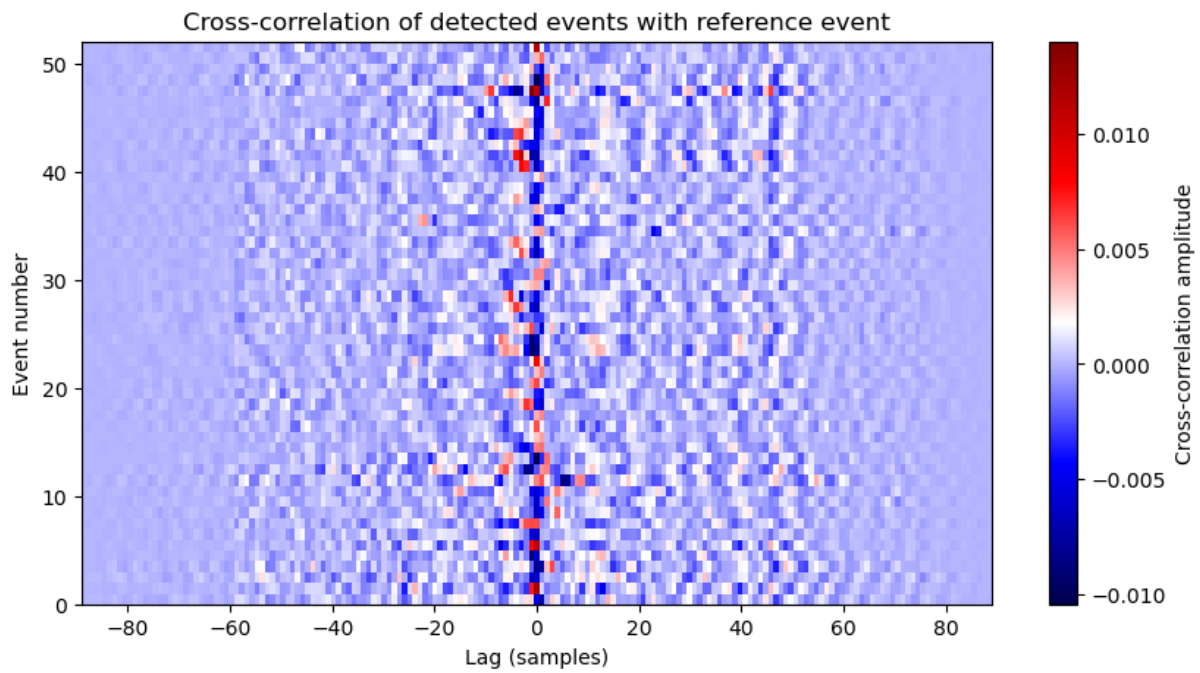


Figure 10 : Cross-correlation function between the first and all the event triggered on FBG 3 located on channel 2 between the October 18th, 2024, and October 26th, 2024.

**Supplementary:** Temperature and strain monitoring in Reykjanes geothermal field, Iceland, using quasi-distributed fiber-optic sensing

Julien Govoorts, Corentin Caudron, Jiaxuan li, Haiyang Liao, Christophe Caucheteur, Yesim Çubuk-Sabuncu, Halldór Geirsson, Vata Hjörleifsdóttir, Kristín Jónsdóttir, Loic Peiffer

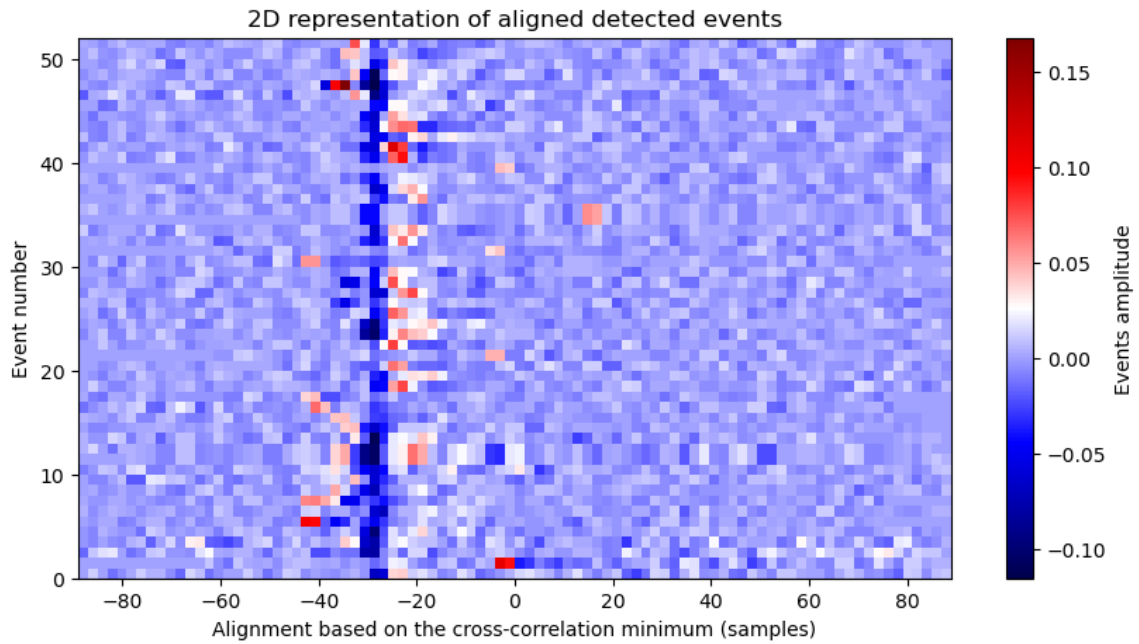


Figure 11 : Aligned events from FBG 3 located on channel 2. The alignment has been performed using the time lag obtained from the cross-correlation function (fig. 10).

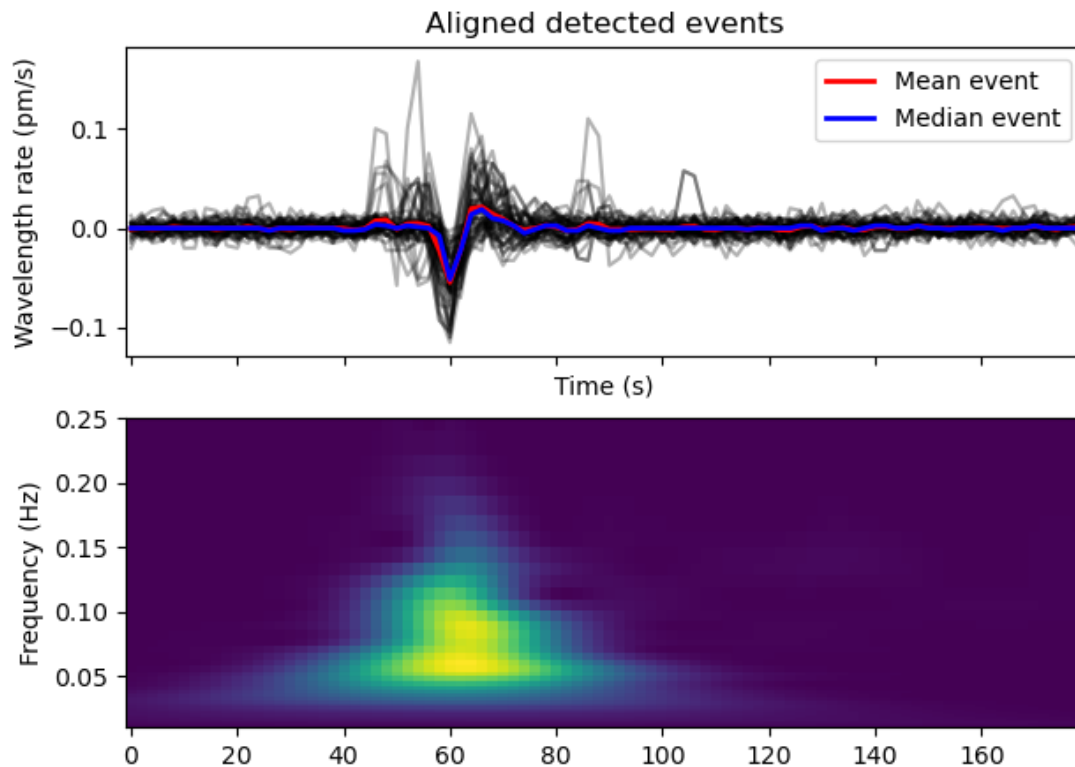


Figure 12 : A. Stacked events of the periodic signal above for the FBG 3 on channel 2. The events were triggered using STA/LTA algorithm. The 90 events were observed and aligned using the time lag determined from the cross-correlation function between the events. Finally, the median and averaged event has been computed. B. Continuous wavelet transform of the mean curve between  $1e^{-4}$  Hz and 0.25Hz.

**Supplementary:** Temperature and strain monitoring in Reykjanes geothermal field, Iceland, using quasi-distributed fiber-optic sensing

**Julien Govoorts**, Corentin Caudron, Jiaxuan li, Haiyang Liao, Christophe Caucheteur, Yesim Çubuk-Sabuncu, Halldór Geirsson, Vala Hjörleifsdóttir, Kristín Jónsdóttir, Loic Peiffer

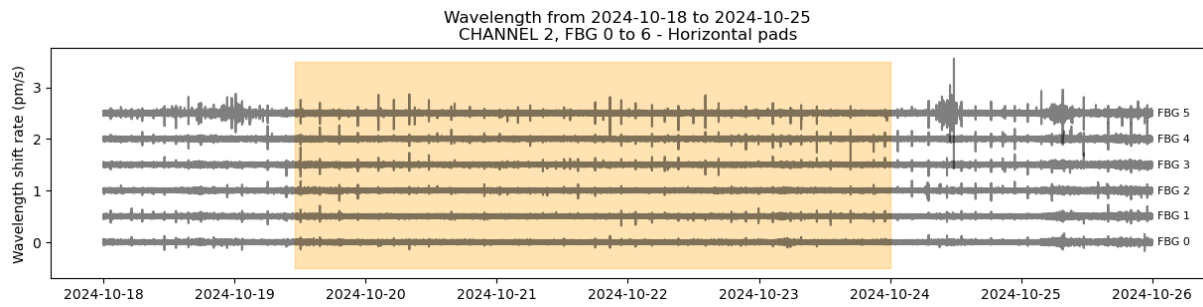


Figure 13 : Time series in strain rate from all the FBG strain-pad located on channel 2 and installed horizontally in-ground between the October 18th, 2024, and October 26th, 2024. The overlaid period is consisting to the range of interest and used for computing the following figures (fig. 14 and 15)

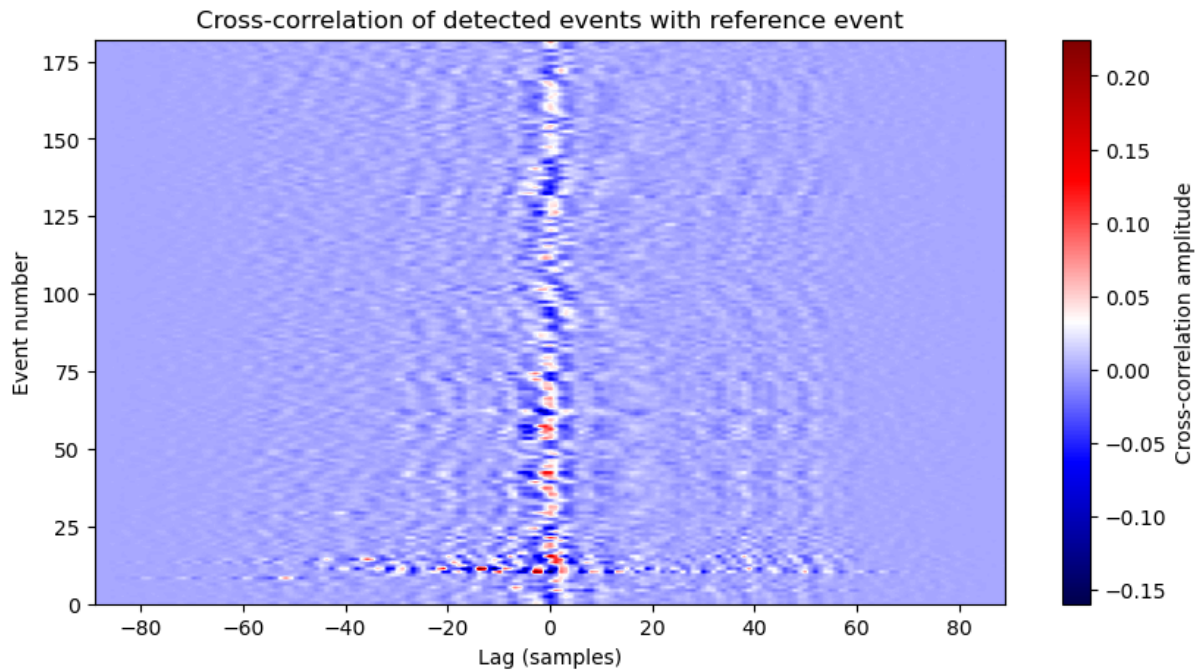


Figure 14 : Cross-correlation functions between the first and all the events triggered in October for all the FBG on channel 2.

**Supplementary:** Temperature and strain monitoring in Reykjanes geothermal field, Iceland, using quasi-distributed fiber-optic sensing

Julien Govoorts, Corentin Caudron, Jiaxuan li, Haiyang Liao, Christophe Caucheteur, Yesim Çubuk-Sabuncu, Halldór Geirsson, Vata Hjörleifsdóttir, Kristín Jónsdóttir, Loic Peiffer

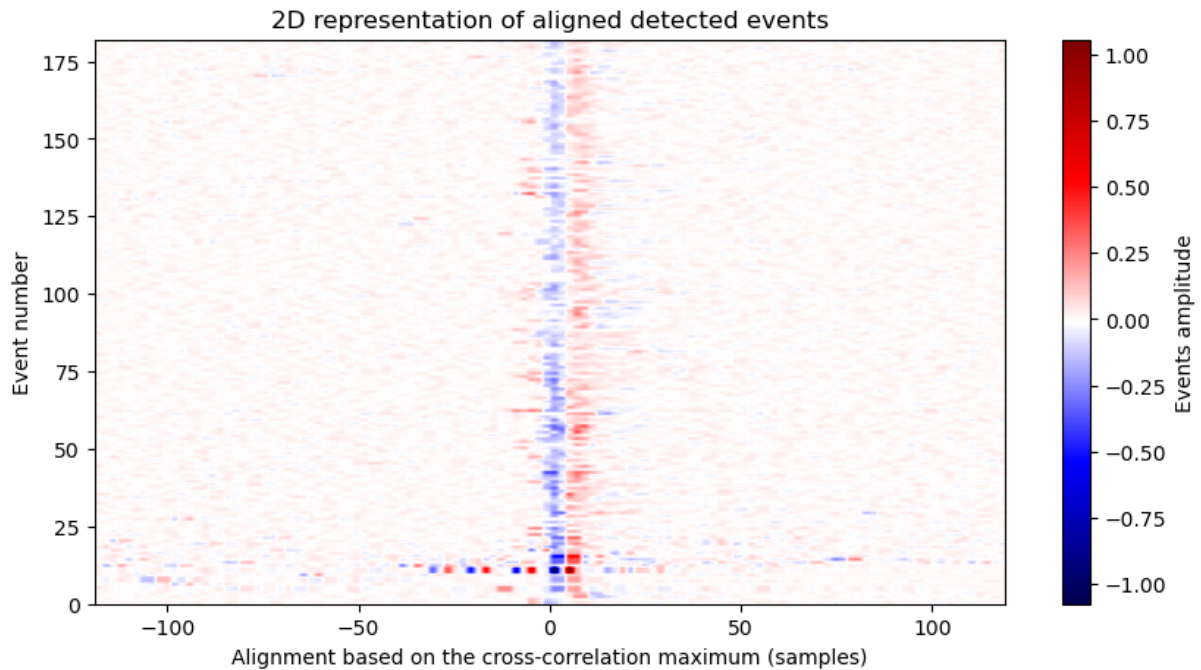


Figure 15 : All the events aligned gathered from all the FBG on channel 2 using the time lag obtained from the cross-correlation in the Fig. 14.

References :

Copernicus Climate Change Service (2023): ERA5 hourly data on single levels from 1940 to present. Copernicus Climate Change Service (C3S) Climate Data Store (CDS), DOI: 10.24381/cds.adbb2d47 (Accessed on 28-APRIL-2026)

Hersbach, H., Bell, B., Berrisford, P., Biavati, G., Horányi, A., Muñoz Sabater, J., Nicolas, J., Peubey, C., Radu, R., Rozum, I., Schepers, D., Simmons, A., Soci, C., Dee, D., Thépaut, J-N. (2018): ERA5 hourly data on single levels from 1940 to present. Copernicus Climate Change Service (C3S) Climate Data Store (CDS), DOI: 10.24381/cds.adbb2d47 , (Accessed on 07-MAR-2023)

Li, J., Biondi, E., Bird, E., & Zhan, Z. (2024). Iceland eruption DAS data [Data set]. CaltechDATA. <https://doi.org/10.22002/tw5s6-nd034>